

Hollow nitrogen atoms probing the jellium edge in front of a Au(111) surface

J. Thomaschewski and J. Bleck-Neuhaus

Universität Bremen, Fachbereich Physik, Kufsteiner Strasse 1, D-28359 Bremen, Germany

M. Grether, A. Spieler, and N. Stolterfoht

Hahn-Meitner-Institut Berlin, Glienicker Strasse 100, D-14109 Berlin, Germany

(Received 13 January 1998)

The deexcitation of slow, hydrogenlike nitrogen ions through interaction with a Au(111) surface is studied by *KLL* Auger electron spectroscopy. Special emphasis is given to processes occurring above the first atomic layer in projectiles that graze the electron gas at different depth. It is found that the increasing electron density around the jellium edge causes acceleration of *L*-shell filling. No difference is seen for projectiles that do or do not penetrate the first atomic layer. A cascade model of hollow atom deexcitation at the border of the electron gas is presented. The model includes a depth dependence of the *L* shell filling rate caused either by interaction with the electron continuum or by a violent collision with a single target atom. Good agreement with experiment is found, along with some evidence for transfer of electrons from states below the Fermi level. [S1050-2947(98)08105-0]

PACS number(s): 79.20.Rf

I. INTRODUCTION

A highly charged ion approaching a metal surface at moderate speed represents an interesting case of multiparticle relaxation [1]. While it is still far outside the electron gas, the ion starts picking up Fermi level electrons into its outer shells with matching binding energy, leaving its inner shells empty. The projectile becomes neutralized stepwise and, thus, is converted to a large “hollow atom” [2]. This process has been confirmed, in quantitative agreement with a classical over-the-barrier (COB) model [3], by measurements of the acceleration of the ion toward the surface. Acceleration takes place until the neutral state is reached and the attraction to its own electrostatic image charge is switched off [4–6].

Since the hollow atom state is still far from equilibrium, further relaxation takes place beginning with an intra-atomic Auger cascade. This cascade is too slow, however, to render the inner shells filled up before the projectile enters the solid [3,7]. The problem of how the filling of the inner shells is influenced by other processes that gain importance when the projectile approaches the electron gas and the lattice atoms of the solid is an interesting one. This question has attracted a lot of discussion (e.g., [7–15]), where frequently a rough distinction was made between processes occurring “above” the surface or “below.”

A typical example is a hydrogenlike first-row-element projectile interacting with a metal surface. Here, considerably fewer *L* Auger electrons are observed than could be expected if the *L* shell were filled by the Auger cascade only. In terms of above-surface processes, the only possible interpretation is that the missing *L* Auger electrons never had been emitted, thus proving a mono-electronic “side feeding” transfer [16] that would reduce the number of Auger transitions needed to fill the *L* shell. An alternate interpretation, based exclusively on below-surface processes, assumes that more *L* Auger electrons indeed had been emitted but subsequently were absorbed by the solid because of their low energy [17]. After accounting for both filling mechanisms, i.e.,

Auger cascading and side feeding, this below-surface picture not only corresponds with the total number of *L* Auger electrons observed, but also with the actual *L* shell population reached by the instant of *KLL* Auger transition. This was confirmed recently for the case of Ne^{9+} projectiles incident on Al [17]. In Ref. [17], side feeding was modeled in a detailed, velocity dependent way [18] based on Landau-Zener and Fano-Lichten mechanisms for electron transfer during close collisions with target atoms. A Monte Carlo model [19] was included for the transport and eventual absorption of the Auger electrons in the solid. In contrast to the detailed description of bulk interactions, the surface itself has been treated in a rather simple way. A single plane was assumed where the solid state interaction of the incident projectile or of the emerging Auger electron suddenly starts or ends, respectively. We note that, even for a closed packed one, the term “surface” may refer to, e.g., the jellium edge, the image plane, the plane of top layer nuclei (taken as $z=0$ in the present paper), or, better, to the whole selvedge region of transition from vacuum to bulk solid.

Recent experiments [20–23] have gone into more detail. These experiments have in common that the ions are given an energy and angle of incidence such that they will graze the electronic border but turn off without penetrating to below the atomic surface. This technique not only reduces the splitting of projectile trajectories into a great variety of different ones penetrating more or less deeply into the solid (see, e.g., [24]), but also selects for observation only those processes occurring above the—fairly equal—heights z_{\min} of the projectile turning points. Moreover, z_{\min} can be moved across the border of the electron gas, by suitably changing incidence conditions. (The z coordinate of the projectile is referred to its nucleus.) Figure 1 sketches the intervening processes.

In a previous paper [20] we have described such experiments with hydrogenlike N^{6+} ions incident on a Au(111) surface. In particular, the outgoing *KLL* Auger electrons were analyzed for angular variations of energy and intensity.

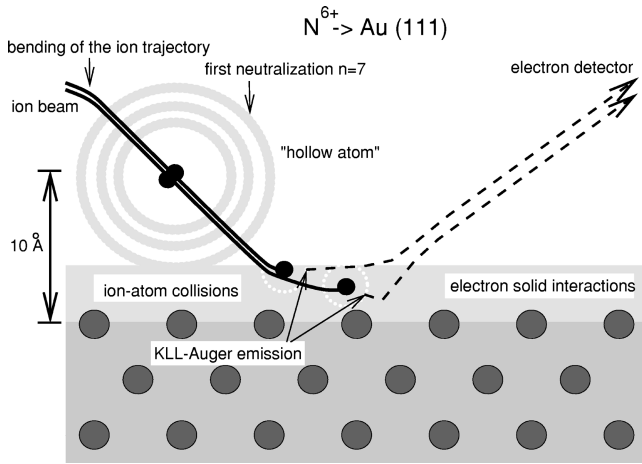


FIG. 1. Processes relevant in the K -Auger emission above the first layer: image acceleration of the incoming ion, formation of a hollow atom, filling of the L shell, electron emission, and electron-solid interaction. The ion enters the electron gas before it is repelled by the surface.

Doppler shift analysis of electron energies showed that a certain fraction of ions emit their KLL electrons on the incoming part of the trajectories and the others on the outgoing (reflected) part. Analysis of transition energies by means of atomic structure calculations further showed that emission on the incoming path predominantly comes from neutral projectiles with minimum possible L shell population for KLL decay, $n_L=2$, thus still forming a type of a ‘‘hollow atom.’’ While in these calculations the remaining four electrons were put into the M shell (or higher), which means energetically already in the conduction band, in reality these electrons will form the screening cloud induced in the surrounding electron gas [25,26]. Emission after reflection is from neutral projectiles too, but with $n_L=3, \dots, 6$ L shell electrons (‘‘filled atoms’’). As a further result, the average z coordinate of the projectiles at emission was derived from the refraction of emitted electrons by the z dependent surface potential. These results are summarized in Fig. 2 where typical trajectories for N^{6+} projectiles incident on Au(111) at (nominally) $\Psi = 10^\circ$ with 165 and 3000 eV kinetic energy are shown together with average projectile positions at KLL emission either as a ‘‘hollow’’ ($n_L=2$) or ‘‘filled’’ ($n_L \geq 3$) atom.

In the present paper we extend this work using the same target, projectile, and incident energies as in Ref. [20]. Now the projectiles are given a vertical velocity gradually increasing from the lowest possible value on, so that they will penetrate more and more deeply into the surface region. Our emphasis is to study the influence of different parts of the surface region on the filling of the hollow atom. It will be shown that filling of the L shell is strongly accelerated when the projectile is about to cross the border of the electron gas, well above the first atomic layer. We will further present an approximative cascade model for the time evolution of this process, based on a z dependent electron transfer rate.

II. EXPERIMENT

Experiments were performed at the 14 GHz ECR source of Hahn-Meitner-Institut (Berlin) using the ultrahigh vacuum

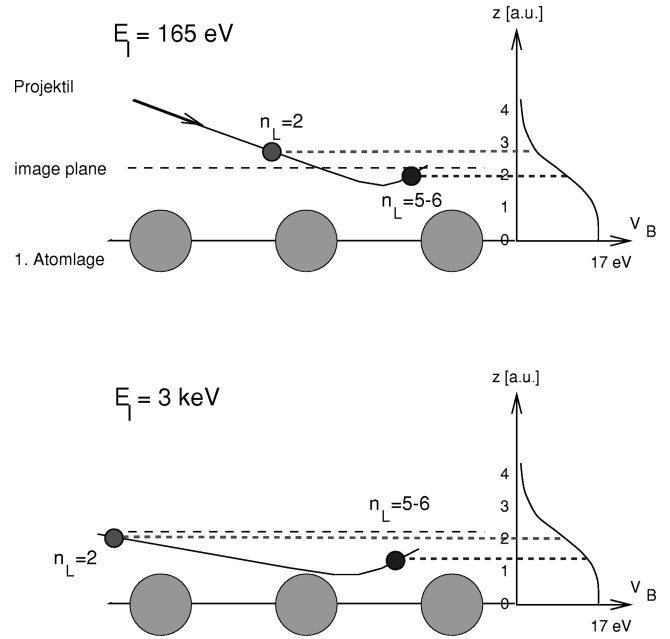


FIG. 2. Sketch of typical N^{6+} ion trajectories not penetrating below the top atomic layer. Average positions of Auger emission from either hollow atom or filled atom configurations are indicated (after Ref. [20]). Right side: potential barrier V_B causing z dependent refraction of the Auger electrons.

chamber of Ref. [27]. A beam of N^{6+} ions prepared at about 60 keV was focused through a deceleration lens system to hit an Au target at (nominally) an energy of 165 eV, 770 eV, or 3 keV and a glancing angle of incidence Ψ ranging from 2.5° to 30° (2.5° to 15° for 3 keV). These angles and energies were chosen so as to provide six different values of the perpendicular velocity component, nominally ranging from 0.9 to 24.0×10^{-3} a.u., in such a way that (approximately) each value occurred several times for different combinations of ion energy and angle of incidence. The image acceleration was calculated according to the COB model [3,28]. Neutralization is completed at $z = 15$ a.u., and the energy gain is then 15.9 eV. The true perpendicular velocity v_{perp} therefore saturates at a lower limit of 6.5×10^{-3} a.u. As a result, the lowest v_{perp} values in the present experiment, whose nominal values still differ by a factor 2, collapse to the narrow interval $6.7 \pm 0.1 \times 10^{-3}$ a.u., while for the highest perpendicular velocity, the nominal and true values used are almost equal.

The set of incidence parameters chosen provides easy control over a wide range of situations beginning from all of the projectiles being repelled above the first atomic layer, and ending up with about 60% penetrating to the 2nd layer or deeper. These figures were obtained in trajectory simulations for a flat Au(111) surface using the MARLOWE [29,30] or our IOR [31,19] codes (see also Sec. IV A). The simulations further show that reflected projectiles had not suffered more than five to six target atom collisions, which are completed in a time of about 500–1000 a.u. (or 12–25 fs).

The target was prepared and held under UHV conditions (2×10^{-8} Pa base pressure). Target preparation and the quality of LEED and Laue pictures obtained in the present experiment were equivalent to those of a surface channeling experiment [32] made before with the same equipment. It is pointed out that surface channeling, seen at ion energies of

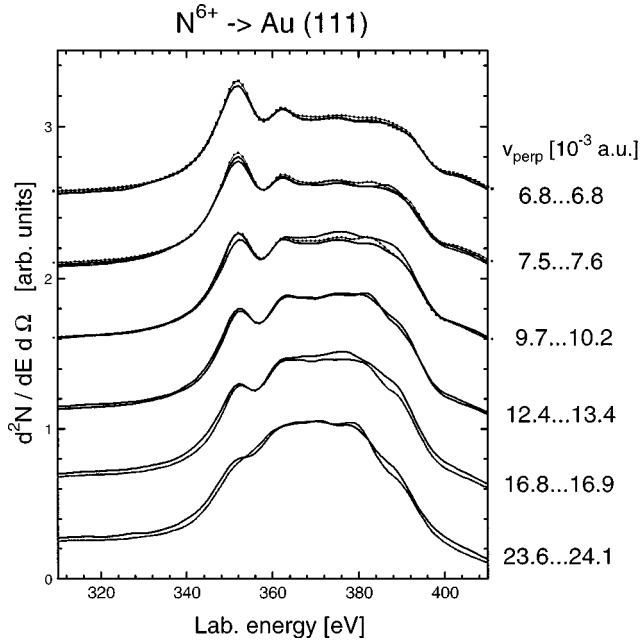


FIG. 3. Auger electron spectra observed in surface normal direction, for ions of 165, 770, and 3000 eV kinetic energy and 2.5° to 30° glancing angle of incidence (nominally). The spectra are arranged in six groups according to the vertical projectile velocity v_{perp} , as shown at the right side (in 10^{-3} a.u., image acceleration included). The spectral shape is strongly dependent on v_{perp} but nearly independent of the ion energy: Notice that the $\approx 30\%$ increase of v_{perp} from group to group causes a stronger systematic change than the up to 16-fold spread of ion energy within a single group.

several keV/amu and extremely flat incidence, demonstrates a surface flatness over about 50 lattice atoms [21], i.e., one order of magnitude more than is needed for our experiment.

Secondary electron spectra were recorded with an electrostatic parallel plate tandem spectrometer of 4.4×10^{-4} acceptance angle, which was set up for 2.6 eV resolution. Spectra were measured from 310 to 410 eV electron energy, i.e., in the region around the broad *KLL* peak. *L* Auger spectra could not be measured with this setup. No background was subtracted. The observation angle was kept constant at the surface normal in order to eliminate any significant effect of z dependent electron refraction. More details of the experimental procedure are given in Refs. [20,27].

Figure 3 shows the spectra obtained. For the purpose of discussion they are arranged in six groups almost homogeneous with regard to their spectral shape. From top to bottom, the narrow low energy structure at 353 eV (and the small structure next at 363 eV), which represents *KLL* emission from an $n_L=2$ state, systematically decreases in relation to the broad remainder, which represents emission from atoms with $n_L \geq 3$ *L* electrons [20]. Since these higher n_L components cannot be resolved in the spectra, we will use the terms ‘‘hollow atom’’ and ‘‘filled atom’’ for the two components with $n_L=2$ and $n_L \geq 3$, respectively.

III. RESULTS AND DISCUSSION

K Auger transitions in hollow atoms

It is seen in Fig. 3 that the grouping according to the amount of *K* Auger emission from hollow atoms is closely

related to the vertical velocity indicated at the right side. We point out that it is important, particularly at slow vertical velocity, to include image acceleration in order to obtain such a narrow one-to-one relationship between v_{perp} and spectral shape. Hence, in the present experiment the perpendicular velocity component governs the electron transfer rate to the *L* shell of N^{6+} projectiles. The faster the projectiles are approaching the surface, the less they contribute as hollow atoms to the total *KLL* Auger emission. This dependence on v_{perp} might support the simple interpretation given in Refs. [10,33] that only the shortening of time for above-surface processes is responsible for the reduction. However, it will be shown below that the weakening of *KLL* emission from hollow atoms is too strong for this explanation. Therefore, a gradual acceleration of the *L* shell filling process at higher v_{perp} must be assumed.

Note that in Fig. 3 each group contains spectra for several ion energies, different by factors about 4 or 16. Spectra shown in the top group were measured with the lower two ion energies. Each of the following two groups comprises spectra of all three ion energies, (nominally) 165, 770, and 3000 eV. The last three groups were measured with the highest two ion energies each. It is seen that the shapes of the spectra are similar for different ion energies within each v_{perp} group but change significantly with v_{perp} from one group to the next. This is in clear contradiction to findings in Ref. [24], where, in contrast to the present experiment, ions were fast enough so that penetration to below the first layer and/or violent scattering by target atoms always occurred.

Another interesting observation refers to the distinction of ions that do or do not penetrate to below the first layer. Only the upper three spectra groups in Fig. 3 belong to situations where all ions are reflected above the first layer. In the bottom group, penetration of about 50% to 60% of the ions occurs. The two groups in between are mixed, i.e., one of the spectra is for nonpenetrating trajectories, the other for 25% and 40% penetration. It is remarkable that the variation of spectral shape, i.e., the filling dynamics of the *L* shell, shows a smooth transition between the regimes of ion penetration and no-penetration. Even the close correlation of spectral shape with the value of v_{perp} holds equally well for all groups, including the mixed ones. This indicates quite clearly that the first atomic layer is not the plane of reference meant in the frequently made division, between narrow low energy Auger peaks emitted ‘‘above surface,’’ and the broad high energy spectrum supposedly emitted ‘‘below’’ [7–15].

The spectra observed allow for a quantitative evaluation of the relation between vertical velocity, v_{perp} , and the amount of *K* Auger emission contributed by hollow atoms, denoted by $f_{n_L=2}$. We note that all spectra seem to be built out of two components of approximately constant shape, with only their relative weights changing from one group to the other. Denoting these two components by $S_{n_L=2}(E)$ and $S_{n_L \geq 3}(E)$, and their weight factors by a and b , we can set the observed spectra $S_{\text{obs}}(E)$ as

$$S_{\text{obs}}(E) = aS_{n_L=2}(E) + bS_{n_L \geq 3}(E). \quad (1)$$

The unknowns [$S_{n_L=2}(E)$, $S_{n_L \geq 3}(E)$, and the v_{perp} dependent a and b] are found in the following way. We first

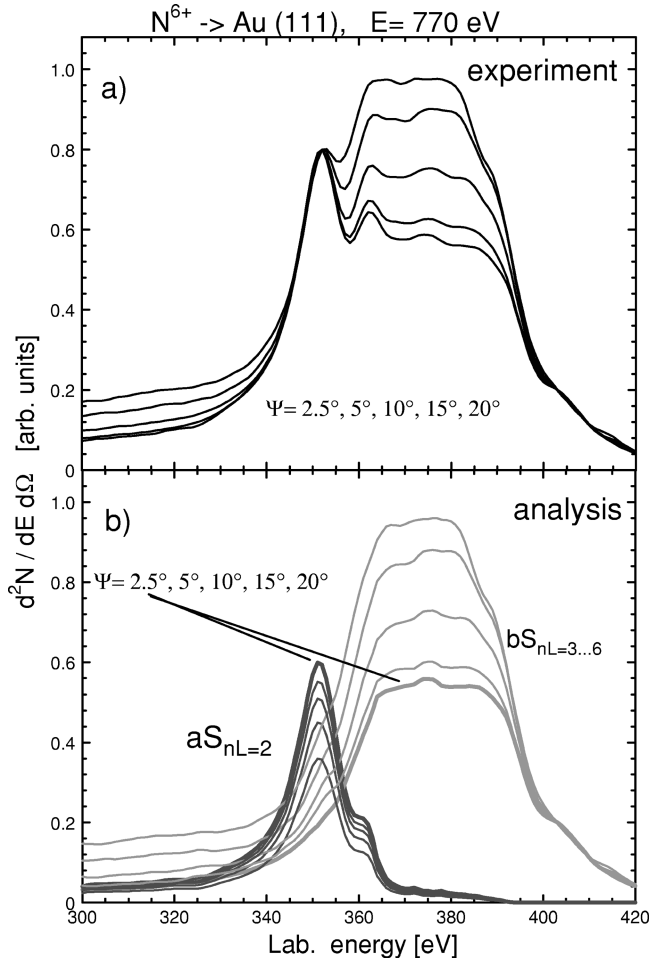


FIG. 4. Deconvolution of *KLL* Auger spectra observed (a) in two components of different weight but approximately constant shape each (b). The narrow component, $S_{n_L=2}$, is from transitions starting from configurations with $n_L=2$ electrons (main peak, $2s^2$; shoulder, $2s2p$). The broad component, $S_{n_L \geq 3}$, indicates transitions from states with $n_L \geq 3$.

guess the shape of $S_{n_L=2}(E)$, guided by the result of atomic structure calculations for $2s^2$ initial configuration with the COWAN code [34,35]. Then we modify this (unique) shape of $S_{n_L=2}(E)$, and adjust the (individual) weight factors a , in order to make all the difference spectra, $bS_{n_L \geq 3}(E) = S_{\text{obs}}(E) - aS_{n_L=2}(E)$, look as similar as possible. To facilitate a detailed comparison with model calculations for

nonpenetrating trajectories (see further below), the spectra for 770 eV ion energy from the first five groups were analyzed in this way. A quite unique deconvolution is achieved as is shown in Fig. 4. Notice the shoulder at 363 eV that had to be added to the original model $2s^2$ spectrum in order to form the $S_{n_L=2}(E)$, which finally yields the nearly constant shapes of the remaining parts $bS_{n_L \geq 3}(E)$ seen in the figure. The shoulder can be identified as the *KLL* transition in hollow atoms where the two L shell electrons are in the $2s2p \ ^3P$ configuration, which cannot decay to $2s^2$ via Coster-Kronig transition [24,33]. The fractional contribution of hollow atoms to *K* Auger emission, $f_{n_L=2}$, is then determined by the fractional area of $aS_{n_L=2}(E)$ in the total spectrum observed, $S_{\text{obs}}(E)$. As a result, $f_{n_L=2}$ gradually changes from 30% for the lowest v_{perp} to 13% for the highest v_{perp} (for nonpenetrating trajectories), as is seen in the 2nd column of Table I.

Since it is not possible to prepare hollow atoms with vertical velocity slower than the limit imposed by the image acceleration, the $f_{n_L=2} = 30\%$ value given in the first row of Table I represents the maximum. This maximum shows good reproducibility for different beam geometries and energies (cf. the top group in Fig. 3). Earlier studies of hollow atom *K* Auger emission from N^{6+} projectiles at Ni, Cu, and Au surfaces resulted in maximum values that were similar [12] and smaller by a factor about 2.5 to 3 [10,11]. Our result confirms the interpretation already suggested [12], namely, that the small values in Refs. [10,11] might be due to local variations in the target surface. Moreover, if the same simple method of spectrum deconvolution that was used in the quoted works were applied to the present spectra, this discrepancy would be smaller. A value even higher than our maximum was reported in Ref. [13] for F^{8+} (*KLL* only) at a conducting *n*-Si surface. In all cases mentioned, this narrow spectral component was addressed as a above-surface contribution, and the broad remainder as a below-surface contribution.

It is evident from Fig. 3 that v_{perp} is a valid parameter to quantify the effectiveness of the L shell filling process. We will now discuss the underlying physical mechanism. According to models presently discussed [26], the solid induces filling of the projectile L shell via mono-electronic electron capture during close collisions with target atoms and via di-electronic or multi-electronic Auger-like transfer from the electron cloud environment. In the first case, the contribution

TABLE I. Contribution $f_{n_L=2}$ of hollow atoms to *KLL* emission—experiment and model calculations (analysis of the spectra of Fig. 3 for nonpenetrating trajectories).

Experiment		Model results				
v_{perp} 10^{-3} a.u.	$f_{n_L=2}$	t_{def} a.u.	c_{min} a.u.	z_{min} a.u.	$f_{n_L=2}$ ($\Gamma_L^f \propto e^{-z/1.2}$)	$f_{n_L=2}$ ($[\Gamma_L^f \propto \rho^{2.1}(z)]$)
6.8	0.30	367	2.3	2.3	0.30	0.29
7.6	0.26	354	2.2	2.1	0.27	0.25
10.2	0.22	304	1.8	1.7	0.21	0.18
13.4	0.17	254	1.5	1.4	0.17	0.15
16.9	0.13	218	1.1	1.1	0.14	0.13

TABLE II. Model calculations for the first three spectra groups in Fig. 3. Each group corresponds to nonpenetrating trajectories of two or three different ion energies but similar v_{perp} . For the definitions of the model parameters, see the text. At each of the model results, the spreading due to different ion energies is indicated. For n_{col} , these intervals overlap largely, in contrast to the other parameters, which show an almost homogeneous correlation to v_{perp} .

Experiment		Model results				
E_{ion} eV	v_{perp} 10^{-3} a.u.	n_{col}	t_{int} a.u.	t_{defl} a.u.	z_{min} a.u.	c_{min} a.u.
165, 770	6.7 ± 0.1	1.2 ± 0.4	1010 ± 10	382 ± 2	2.3 ± 0.1	2.4 ± 0.1
165, 770, 3000	7.5 ± 0.1	2.3 ± 1.1	940 ± 30	364 ± 10	2.0 ± 0.1	2.2 ± 0.1
165, 770, 3000	9.9 ± 0.2	2.8 ± 1.5	780 ± 50	317 ± 13	1.6 ± 0.1	1.9 ± 0.2

of K Auger emission from hollow atoms would diminish with an increasing number of collisions, sufficiently violent to provoke Fano-Lichten or Landau-Zener electron transfer processes. In the second case, we would expect to see this contribution diminish with increasing conduction electron density surrounding the projectile. In order to gain more detailed insight into the importance of these parameters, further evaluation is based on model calculations.

IV. MODEL CALCULATIONS

A. Ion trajectory model

Extended simulations of trajectories were made using our IOR code [31,19], which allows detailed time dependent analysis of projectile history. For the ion-ion potential, the original ZBL formula [36] was used, because in Ref. [20] it was shown that the calculated trajectories fit well to the detailed scenario, deduced from experiment, for the spatial regions of K emission (see Fig. 2). The code integrates the Newtonian equation of motion of the incident particle under the summed interaction potentials of all lattice atoms at sites closer than $1.5d$ (d is the next neighbor distance in the lattice). However, if in the course of its trajectory the projectile approaches closer than $d/2$ to one of the lattice atoms, the code switches over to the mode of binary collision in the center of mass system, thus taking full account of recoil effects, until a distance $>d/2$ is reached again. During the binary collision mode, the remainder of the lattice is neglected if the recoil energy is sufficient to produce a vacancy, otherwise the recoiling target atom is assumed to suffer an elastic reflection by the lattice, at the instant of closest approach of the projectile. For further details, see Refs. [31,19].

Calculations were performed for incidence conditions of nonpenetrating projectiles only (i.e., for all spectra shown in the first three groups in Fig. 3, and for the spectra at 770 eV and 3000 eV ion energy in the 4th and 5th group, respectively). Under these conditions, the trajectories approach the top layer, depending on v_{perp} , down to $z_{\text{min}} = 2.3, \dots, 1.1$ a.u. A variety of quantities were calculated and checked for a correlation with v_{perp} that would help to understand the variation of L shell filling. These are as follows.

n_{col} : the number of collisions closer than 2.7 a.u., i.e., where the projectile L shell and the target atom $5d$ or $5p$ shells begin to overlap.

t_{int} : the time spent by the projectile within a region ‘‘close to the surface,’’ which was defined by the limit z

$= 4.8$ a.u. This is the position where the COB model predicts occupation number $n_L = 1$ for the incoming nitrogen projectile, and is also the limit of validity for this classical model [3].

t_{defl} : the ‘‘travel-in time window,’’ i.e., the time spent by the projectile on its way in before it is deflected. This was estimated as the time needed to travel at constant v_{perp} from the same limit $z = 4.8$ a.u., to z_{min} . (We recall that it was shown from Doppler shift measurements that hollow-atom K Auger emission mainly occurs before the projectile is deflected [20]. Hence, t_{defl} is an upper limit for the time window for capturing the second L electron and making the hollow-atom KLL transition.)

z_{min} : the minimum z coordinate reached at the turning point.

c_{min} : the minimum internuclear distance ever reached to a target atom.

In Table II we give the results for the trajectories of the first three groups of Fig. 3, each group being built out of spectra from nonpenetrating projectiles of two or three different energies but almost the same v_{perp} . The results indicate that all five parameters are related to the vertical velocity in the average, but that the additional influence of ion energy is significantly bigger for n_{col} than for the other four. This can be seen from the uncertainty limits given in the table, which reflect the variation of the calculated results with ion energy. For n_{col} (see the 3rd column of Table II) these intervals overlap largely, i.e., the numbers n_{col} vary stronger *within* each group rather than from one group to the next. It follows that spectra selected for a certain number of close collisions would have any one of the shapes seen in the upper half of Fig. 3, i.e., they would correspond to quite different amounts of L shell filling. A proportionality of L shell filling rate and collision rate was observed for Ne^{9+} projectiles in Al [18]. For the present case, however, the number of close collisions with target atoms is not a factor important for the filling of the L shell.

The time parameters (columns 4 and 5 in Table II) cannot explain the observations either. From the first to the third line, the close-to-surface time t_{int} decreases, but, in spite of this shortening of interaction time, a higher degree of L shell filling is achieved. Hence, the variation of t_{int} is contrary to the explanation tentatively looked for. In contrast, the travel-in time t_{defl} varies in the correct sense: in accordance with the decrease of $f_{n_L=2}$, the time window open for cap-

ture of the 2nd L electron and the subsequent hollow-atom K Auger emission is gradually shortening. This behavior is found for all five cases of nonpenetrating trajectories (see also the 3rd column of Table I). However, the overall shortening is 150 a.u. only. This is too little, considering that the time constant of the hollow atom KLL decay is estimated as 430 a.u. [24]. Not even half of the observed reduction of $f_{n_L=2}$ could be explained by this shortening of the “time window for observation” (see [33]) even if the waiting time for the second L shell electron were neglected. We conclude that the suppression of the hollow atom contribution to K Auger emission indicates an acceleration of electron transfer to the L shell already active long before the projectile is deflected.

The remaining two parameters, z_{\min} and c_{\min} , show an equally close relation to v_{perp} and, therefore, to the contribution of hollow atoms to K Auger emission. It is noted that the variation of both these parameters corresponds to a considerable increase of the maximum of electron density reached by the projectile. If the jellium model is adapted for the Au conduction band [37], the upper value $z_{\min}=2.3$ a.u. corresponds to the jellium edge where the electron density is 50% of the bulk value, while at the lower $z_{\min}=1.1$ a.u., about 80% of the bulk density is reached. Similarly, the c_{\min} range corresponds to a still increasing overlap of the projectile L shell with radius 0.7 a.u. and the full Au $5d$ and $5p$ shells, of radii 1.1 and 0.8 a.u. [38] approximately. That means that, although in the present experiment the L shell filling observed is not related to the *number* of close collisions (<2.7 a.u.), the minimum internuclear distance reached in the most violent one of them may still be a decisive factor for the amount of L shell filling achieved by the instant of K Auger transition.

B. Deexcitation cascade model

The picture obtained so far of the deexcitation process of N^{6+} up to the filling of its K shell hole allows for a detailed analysis by means of a cascade model. Such models have been worked out previously by Burgdörfer *et al.* for the vacuum region farther above the image plane (COB model, Ref. [3]), and by Page *et al.* [19], Stolterfoht *et al.* [18], and Limburg *et al.* [24], for projectiles penetrating into the bulk solid. As mentioned above, the surface model used was that of a single plane where the bulk interactions are abruptly switched on or off.

An improved treatment of the surface region, such as is needed for experiments with projectiles only grazing the electron gas, was proposed by Burgdörfer *et al.* [38], who extrapolated the COB model down to $z=0$. We will try here a different approach in the opposite direction, i.e., by stepwise incorporating conditions characteristic for the surface region into the models originally developed for bulk solid. Even though the results will still be quite approximate, we expect to see the increase of hollow atom contribution to K Auger emission, observed with projectiles penetrating shallower into the electron gas (cf. Table I). Furthermore, we expect to find agreement with the observation [20] that under the present conditions the K Auger emission from hollow and filled atoms occurs before or after the projectiles are reflected at the surface, respectively, but always in the vicinity

of the jellium edge. That means that the K Auger transition occurs either during the travel-in-time t_{defl} or later in the second half of the close-to-surface time interval t_{int} as given above, respectively. For the initial condition of our cascade model we choose the starting point of these time intervals, i.e., when the projectile crosses the distance $z=4.8$ a.u. having $n_L=1$ electron in the L shell, according to the COB model.

The time development is obtained from rate equations for the number of projectiles $N_{n_L}(t)$ carrying n_L electrons in their L shell and one hole in their K shell [18]:

$$\frac{dN_{n_L}}{dt} = \Gamma_{L,n_L-1}^f N_{n_L-1} - \Gamma_{L,n_L}^f N_{n_L} - \Gamma_{K,n_L} N_{n_L}. \quad (2)$$

Here, the first term represents the increase of the n_L population due to electron transfer at a filling rate Γ_{L,n_L-1}^f , which is given by the sum of the collisional capture rate Γ^c , and the rate of Auger-like transitions, Γ_L :

$$\Gamma_{L,n_L-1}^f = \Gamma_{L,n_L-1}^c + \Gamma_{L,n_L-1}. \quad (3)$$

The two loss terms in the rate equation (2) represent the step to next higher n_L and the K Auger decay from which, finally, the quantity $f_{n_L=2}$ and the mean emission times for hollow and filled atoms are calculated for comparison with experiment.

We note that the experimental results give direct evidence that the K Auger lifetimes for hollow and filled atom configurations fall in between t_{defl} and t_{int} , approximately. In order to fit to $f_{n_L=2}$ values observed, the K Auger lifetime of the hollow atom state must be of the order of the time window t_{defl} . The K Auger lifetimes of the more filled atom states must be shorter than t_{int} , so that in any case the KLL transition can be completed within this time interval. Thus, Γ_{K,n_L} can depend on n_L quite weakly only. A strong increase of Γ_{K,n_L} , be it linear in n_L as assumed for Ne projectiles in current cascade models [17–19], or even quadratic as assumed, e.g., for Ar [39], can be excluded for N.

We therefore adopt the K Auger rates [24] calculated with the COWAN codes [34,35] for neutral nitrogen configurations with n_L ranging from 2 to 6. The corresponding lifetimes vary between 417 and 570 a.u. only and therefore fit well to our scenario for the deexcitation cascade. As to the L shell filling rates, the experiment shows that they are fast enough to open *and* to close the channel for K Auger emission with $n_L=2$, within the time window t_{defl} . Moreover, the variation of $f_{n_L=2}$ indicates that L shell filling rates significantly increase for deeper grazing trajectories. A rough estimate shows that the transfer rates, particularly for the first two steps creating and destroying the $n_L=2$ configuration, have to increase about twofold to threefold effectively from top to bottom of Table I. This is a quite strong variation, considering that the grazing depth z_{\min} (or c_{\min}) varies by 1.2 a.u. only.

A depth dependent transfer rate is a well known phenomenon in surface interactions of singly or doubly charged ions [40], and for highly charged ions, too [39]. Frequently the z dependence is approximated by

$$\Gamma_{L,n_L}^f = \Gamma_0^f \exp(-z/\lambda) \quad (z > 0). \quad (4)$$

The bulk rate Γ_0^f and the decay length λ will first be treated as fit parameters and later compared to theoretical estimates. It is outside the scope of the present paper to develop a time dependent model for the variation of the transfer rate along the projectile's trajectory. Considering that the projectiles spend most of their time in the vicinity of z_{\min} , where the rate is maximum, we will take the rate at z_{\min} as a constant value valid throughout the whole trajectory within the close-to-surface region $z < 4.8$ a.u.

With these approximations we find good agreement between experiment and cascade model (2nd and 5th column of Table I), if fit values $\lambda = 1.2$ a.u. and $\Gamma_0^f = 1/28$ a.u. are used. This λ value fits well to the qualitative argument given above regarding the strong z dependence of the rates. However, it is considerably less than the estimated 1.6 a.u. which can be obtained from the well known formula $\lambda = (2E_B)^{-1/2}$ [40] for electron capture from the Fermi level when the Au work function (5.2 eV) is used for the binding energy E_B . Although the formula is thought to be valid mainly for z above the jellium edge, the stronger z dependence found in our experiment may be taken as an indication of a certain participation of electrons from states below the Fermi level. Indeed, at distances reached here, collisional electron transfer from Au $5d$ and $5p$ shells (with binding energies around 13 and 54 eV) will contribute to side feeding in a z_{\min} dependent way. This process, however, is not easily incorporated quantitatively into the model: First of all, it was shown above that it is not the number (or rate) of these close collisions that is important here, but rather the most violent one of them. Moreover, a serious disagreement is noted in relation to another estimate of λ , valid for the case of side feeding into a deeply lying orbital [39]. This estimate is based on the sum of the respective orbital radius and the z coordinate of the jellium edge, i.e., $\lambda = 3$ a.u. here, a value by far too large for the present experiment. It is suggested, therefore, that quantitative estimates of collisional electron transfer probabilities be based on complete molecular orbital calculations for the (hollow-)N-Au system, which still have to be worked out (see, e.g., Ref. [41]).

Regarding absolute filling rates we note that our ‘‘bulk’’ value [Γ_0^f in Eq. (4)] found in the fit is close to the $1/36$ a.u. obtained theoretically [42,43] for the *LCV* process at a hollow N atom in the conduction electron gas of bulk Au. This motivates us to try, in a second approach, an extrapolation of this mechanism toward the region of decreasing electron density at the border of the electron gas. In the *LCV* process an electron is captured from the screening cloud *C* into the projectile *L* shell while the excess energy is transferred to the electron gas *V*. Here this energy mainly appears in the form of a single electron excitation, thus giving rise to Auger-like electron emission. The shape of the screening cloud in an infinite medium has recently been calculated [25,26] by means of nonlinear density functional theory. The cases studied were Ne ions embedded in electron gases whose densities ρ_0 just match those of the Au conduction band in the bulk solid and at the jellium edge. It is shown in Ref. [26] that the screening cloud has a density maximum that not only exceeds the background density by several times, but is even

higher and closer to the nucleus than the atomic *M* shell maximum in an isolated hollow atom. It also was pointed out in Ref. [26] that the reduction of background density ρ_0 has little influence on the shape of the cloud. This resembles the behavior of linear Thomas-Fermi screening, which varies as $\rho_0^{(1/6)}$ only [38]. The weak dependence on ρ_0 also provides qualitative understanding of the quite effective screening at much lower electron density, e.g., in the tail of the electron gas (at $z \approx 4, \dots, 6$ a.u., i.e., even extending into the range where the classical COB model is applied), as it was inferred from measurements of charge state distribution of multiply charged projectiles after surface channeling [21,23]. We therefore assume the screening cloud present during the whole close-to-surface time t_{int} of the projectile.

From this picture one might expect a weak variation of the *LCV* rate with electron density like, e.g., $\Gamma_{L,n_L} \propto \rho_0^k$ with an exponent k probably less than 1. However, rates calculated for a hollow N atom in electron gases of the interesting densities can be approximated roughly with an exponent k around 1.5. We will take k as a parameter to fit. The shape of the jellium edge can be modeled (Ref. [44]) as a tanh-like soft step with 1.5 a.u. thickness parameter. In the spirit of a local density assumption, we will adjust $\Gamma_{L,n_L}^{\text{Au}}$, as given in Ref. [42] for bulk Au, to the electron density $\rho(z)$ felt by the projectile at height z . Again, we will take the rate at z_{\min} for the whole trajectory below $z < 4.8$ a.u. It is noted that the problem of spatial inhomogeneity of electron density across the diameter of the projectile *L* shell is neglected here, although the inhomogeneity is considerable when z (i.e., the projectile's nucleus) is close to the jellium edge. Hence,

$$\Gamma_{L,n_L} = \left(\frac{\rho(z_{\min})}{\rho^{\text{Au}}} \right)^k \Gamma_{L,n_L}^{\text{Au}}. \quad (5)$$

In order to see the possible magnitude of effects induced by the z dependent electron density, we try this part of the model alone, neglecting for the moment all collisional capture rates Γ^c in the model equations (3). Surprisingly good results can be obtained again (cf. the last column of Table I). However, k has to be given a value 2.1, and the bulk rates $\Gamma_{L,n_L}^{\text{Au}}$ have to be reduced by 30% below the theoretical values. The large k means stronger dependence on the electron gas density than is expected according to the continuum theory of the *LCV* process. This again may be taken as a hint towards participation of deeper bound electrons.

The cascade model also yields average times of Auger emission from hollow or filled atoms as well as z distributions of emission sites. The calculations [based on either filling model Eqs. (4) and (5)] show that emission from a hollow atom occurs in the average before the ion is deflected, and emission from a filled atom occurs afterwards. Hence, good agreement is achieved with the scenario previously deduced from Doppler shift analysis of measured spectra [20]. Also, the calculated average emission height agrees well with the data obtained from the z dependent refraction effect on the emitted Auger electrons. It is seen that the scenario suggested in our previous work [20] (reproduced here in Fig. 2) is confirmed by the time dependent analysis outlined above.

We notice that the L shell filling of slow N^{6+} projectiles at the border of the Au conduction band can be reproduced using a cascade model based on interaction with the conduction electrons, either via resonant electron transfer or via LCV transition. In both cases, however, quantitative fitting of the model requires us to take parameter values that indicate some contribution of deeper bound core electrons. (This observation remains true even in a combined model made out of both the mechanisms discussed above.) These core electrons most likely are transferred resonantly in the single collision achieving the minimum internuclear distance between projectile and target. Individual contributions of different transfer processes cannot be determined further from our measurements of K Auger electrons alone. To solve this problem (and to test our extrapolation of the recent continuum theory) it is suggested to observe simultaneously the low energy electrons eventually emitted after LCV excitation of the conduction band.

V. SUMMARY

We study the deexcitation of hollow N atoms that slowly approach a solid Au(111) surface with a hole in their K shell. In particular, the filling state of the L shell by the instant of KLL Auger transition is examined by means of secondary electron spectroscopy. Projectile trajectories are adjusted to graze more or less deeply the electronic surface only, or to penetrate the crystal lattice too. The spectra show that for the low projectile energies used here (165–3000 eV), the vertical velocity component is the parameter that practically alone determines the L shell filling. The question of penetration of the first atomic layer does not show up. The distinction traditionally made between above- and below-surface emission of inner shell Auger electrons in the relaxation process of highly charged ions cannot be associated, therefore, with the

plane of the first atomic layer. In the present experiment, significant acceleration of L shell filling already occurs when the projectile passes through the region of increasing electron density $\rho(z)$ around the jellium edge. It is shown by means of trajectory simulations that the variation of L shell filling is not related to the number of close collisions with target atoms. A cascade model for the L shell filling process above the first atomic layer is presented. The L shell filling rate is modeled with a z dependence like that expected for electron capture from the conduction band. Two possible transfer mechanisms are considered: resonant transfer and Auger-like LCV transition, involving the screening cloud formed in the tail of the electron gas. As a result, all experimental findings, including average times and positions of KLL Auger emission, are well reproduced with both transfer mechanisms. However, in both cases the fitted parameter values indicate a certain participation of deeper bound electrons. Further clarification of the contributions from each of these mechanisms can be expected if electrons emitted in the LCV process are observed directly.

The whole picture derived is in agreement with the scenario obtained in previous work [20], based solely on the analysis of emerging K Auger electrons and their solid state interactions after their emission in the surface region above the first layer. This leads us to the conclusion, regarding both the filling dynamics of incoming hollow atoms and the solid state interactions of outgoing Auger electrons, that the most appropriate meaning of “surface” in the deexcitation of slow, multicharged nitrogen ions at a gold surface is the border of the electron gas.

ACKNOWLEDGMENT

We thank C. Lemell for help with the COB calculations.

-
- [1] A. Arnau *et al.*, Surf. Sci. Rep. **27**, 113 (1997).
 - [2] J. P. Briand *et al.*, Phys. Rev. Lett. **65**, 159 (1990).
 - [3] J. Burgdörfer, P. Lerner, and F. W. Meyer, Phys. Rev. A **44**, 5674 (1991).
 - [4] H. Winter and C. Auth, Nucl. Instrum. Methods Phys. Res. B **90**, 216 (1994).
 - [5] F. Aumayr *et al.*, Phys. Rev. Lett. **71**, 1943 (1993).
 - [6] C. Lemell *et al.*, Phys. Rev. A **53**, 880 (1996).
 - [7] F. W. Meyer *et al.*, Phys. Rev. Lett. **67**, 723 (1991).
 - [8] H. J. Andrä *et al.*, Z. Phys. D **21**, S135 (1991).
 - [9] J. Das, L. Folkerts, and R. Morgenstern, Phys. Rev. A **45**, 4669 (1992).
 - [10] J. Das and R. Morgenstern, Phys. Rev. A **47**, R755 (1993).
 - [11] F. W. Meyer, C. Havener, and P. A. Zeijlmans van Emmichoven, Phys. Rev. A **48**, 4476 (1993).
 - [12] F. W. Meyer *et al.*, Phys. Rev. A **48**, 4479 (1993).
 - [13] H. J. Andrä *et al.*, Europhys. Lett. **23**, 361 (1993).
 - [14] J. Bleck-Neuhaus *et al.*, Phys. Rev. A **49**, R1539 (1994).
 - [15] R. Köhrbrück *et al.*, Phys. Rev. A **50**, 1429 (1994).
 - [16] L. Folkerts and R. Morgenstern, Europhys. Lett. **13**, 377 (1990).
 - [17] M. Grether, D. Niemann, A. Spieler, and N. Stolterfoht, Phys. Rev. A **56**, 3794 (1997).
 - [18] N. Stolterfoht *et al.*, Phys. Rev. A **52**, 445 (1995).
 - [19] R. Page *et al.*, Phys. Rev. A **52**, 1344 (1995).
 - [20] J. Thomaschewski *et al.*, Nucl. Instrum. Methods Phys. Res. B **125**, 163 (1997).
 - [21] F. W. Meyer, L. Folkerts, and S. Schippers, Nucl. Instrum. Methods Phys. Res. B **100**, 366 (1995).
 - [22] F. W. Meyer, L. Folkerts, H. Folkerts, and S. Schippers, Nucl. Instrum. Methods Phys. Res. B **98**, 441 (1995).
 - [23] Q. Yan, D. M. Zehner, F. W. Meyer, and S. Schippers, Phys. Rev. A **54**, 641 (1996).
 - [24] J. Limburg *et al.*, Phys. Rev. A **51**, 3873 (1995).
 - [25] A. Arnau *et al.*, Phys. Rev. A **51**, R3399 (1995).
 - [26] N. Stolterfoht *et al.*, Nucl. Instrum. Methods Phys. Res. B **124**, 303 (1997).
 - [27] M. Grether, A. Spieler, R. Köhrbrück, and N. Stolterfoht, Phys. Rev. A **52**, 426 (1995).
 - [28] J. Burgdörfer and F. W. Meyer, Phys. Rev. A **47**, R20 (1993).
 - [29] M. T. Robinson and I. M. Torrens, Phys. Rev. B **9**, 5008 (1974).

- [30] M. T. Robinson, Phys. Rev. B **40**, 10 717 (1989).
- [31] J. Bleck-Neuhaus, R. Page, and A. Saal, Nucl. Instrum. Methods Phys. Res. B **78**, 113 (1993).
- [32] A. Hoffknecht, Master's thesis, Universität Osnabrück, 1996.
- [33] S. Schippers *et al.*, Phys. Rev. A **50**, 540 (1994).
- [34] R. D. Cowan, *The Theory of Atomic Structure and Spectra* (University of California Press, Berkeley, 1981).
- [35] S. Schippers, User's Guide to COWAN-Utilities, Vers. 4.0, KVI Internal Report KVI-189i, Groningen, 1994.
- [36] J. F. Ziegler, J. P. Biersack, and U. Littmark, *The Stopping and the Range of Ions in Matter* (Pergamon, New York, 1985).
- [37] N. V. Smith, C. T. Chen, and M. Weinert, Phys. Rev. B **40**, 7565 (1989).
- [38] J. Burgdörfer, C. Reinhold, and F. Meyer, Nucl. Instrum. Methods Phys. Res. B **98**, 415 (1995).
- [39] S. Winecki, C. L. Cocke, D. Fry, and M. P. Stöckli, Phys. Rev. A **53**, 4228 (1996).
- [40] A. Niehaus, in *Ionization of Solids by Heavy Particles*, edited by R. Baragiola (Plenum Press, New York, 1993), p. 79.
- [41] C. C. Havener *et al.*, Radiat. Eff. Defects Solids **109**, 99 (1988).
- [42] R. Diez-Muñoz *et al.*, Phys. Rev. Lett. **76**, 4636 (1996).
- [43] R. Diez-Muñoz *et al.* (unpublished).
- [44] N. D. Lang and W. Kohn, Phys. Rev. B **7**, 3541 (1973).